Telomere dysfunction and inactivation of the p16^{INK4a}/Rb pathway in pyothorax-associated lymphoma

Kristianti Tresnasari,[1] Tetsuya Takakuwa,[1,3] Maria Francisca Ham,[1] Nur Rahadiani,[1] Hiroo Nakajima[2] and Katsuyuki Aozasa[1]

[1]Department of Pathology and [2]Department of Radiation Biology and Medical Genetics, Osaka University Graduate School of Medicine, Osaka 565-0871, Japan

(Received November 6, 2006/Revised January 31, 2007/2nd Revised February 28, 2007/Accepted March 4, 2007/Online publication April 13, 2007)

Previous studies have indicated that genome instability is involved in the lymphomagenesis of pyothorax-associated lymphoma (PAL), which develops in patients with a long-standing history of pyothorax. One of the well-known causes of genome instability is telomere dysfunction. In the present study, the condition of telomeres was analyzed in the cell lines and clinical samples from PAL. Telomere length (TL) in PAL cell lines was extremely short (<4.5 kbp). TL in tumor samples was broad in range, and shorter than that in the peripheral blood leukocytes from the matched patients. Three of five PAL cell lines showed frequent loss of telomere signals (telomere erosion); however, telomerase activity in PAL cell lines was similar to that in Burkitt lymphoma cell lines. Rb expression was detected in three PAL cell lines and four of 15 clinical samples, respectively. Rb protein expressed in three PAL cell lines was heavily phosphorylated, indicating that function of Rb protein was suppressed. p16^{INK4a} expression was not detected in either cell lines or clinical samples. The promoter region in p16^{INK4a} was heavily methylated in all cell lines as well as the clinical samples. Inactivation of the p16^{INK4a}/Rb pathway may allow continuous cell division and critical telomere shortening, which induce genome instability, finally leading to malignant transformation. Taken together, telomere dysfunction and inactivation of the p16^{INK4a}/Rb pathway might play a role for PAL development. (*Cancer Sci* 2007; 98: 978–984)

Non-Hodgkin lymphoma frequently develops in the pleural cavity of patients with long-standing pyothorax resulting from artificial pneumothorax for the treatment of pulmonary tuberculosis or tuberculous pleuritis.[1] This tumor stand as a distinct clinicopathological entity, thus the term pyothorax-associated lymphoma (PAL) has been proposed by Dr Aozasa for this type of tumor.[2] PAL is now listed as a distinct disease entity in the recent World Health Organization Classification of tumors.[3] PAL consists mostly of diffuse large B-cell lymphoma, and is strongly associated with EBV infection.[1] PAL patients might have long been treated with drugs against underlying lung tuberculosis, antibiotics, or exposed to bacterial or viral products, and frequent diagnostic radiation for the appropriate employment of artificial pneumothorax and pyothorax. These factors might cause DNA damage in cells present in chronic pyothorax lesions. Indeed established cell lines from PAL have highly complex karyotypes, indicating the presence of genome instability.[4,5]

Telomeres are nucleoprotein complexes located at the end of eukaryotic chromosomes.[6] They have essential roles in preventing terminal fusions, protecting chromosome ends from degradation, and chromosome positioning in the nucleus. These terminal structures consist of a tandemly repeated DNA sequence (TTAGGG in vertebrates) that varies in length from 5 to 15 kb in humans.[7] Progressive telomere shortening occurs along with the division of primary human cells, thus activating tumor suppressor pathways through triggering senescence and inhibiting tumorigenesis.[8] Senescence can be defined as a state of permanent growth arrest, in which cells enter into the G0/G1 phase of the cell cycle, take an enlarged, flattened morphology, exhibit an altered pattern of gene expression, and yet remain metabolically active. The activation of p14^{ARF}/p53 and p16^{INK4a}/Rb pathways is important for tumor suppressor mechanism in human cells at telomere shortening.[9] Inactivation of these pathways allows cells to continuous division despite an increase in telomere dysfunction, and finally to enter into telomere crisis. Recent data suggest that the severe genome instability that is present during telomere crisis promotes secondary genetic changes that facilitate carcinogenesis.[10–12] Reactivation of telomerase is important in the stabilization of telomere ends and allows continuous tumor growth.[13]

In the present study, it was shown that most of the PAL cell lines had short telomeres with frequent telomere erosion, while telomerase was reactivated. The p53 and p16^{INK4a}/Rb tumor suppressor pathways were abrogated in the cell lines and clinical samples from PAL. These findings suggest a role of telomere dysfunction and inactivation of the p16^{INK4a}/Rb pathway in PAL development.

Materials and Methods

Cell lines. Six cell lines, OPL-1, -2, -3, -4, -5, and -7 were established from six patients with PAL, who had a 39–66-year history of chronic pyothorax resulting from artificial pneumothorax for the treatment of pulmonary tuberculosis or tuberculous pleuritis. Their characteristics have been reported previously.[4,5] Pal-1 and Deglis established from PAL patients were a kind gift from Dr. Daibata and Dr. Al Saati, respectively.[14,15] All PAL cell lines were positive for the EBV genome using Southern blotting and EBER-1 expression using *in situ* hybridization.[4,5,14,15] A lymphoblastoid cell line, IB-4, was used as a control, which was a kind gift from Dr. E Kieff.[16] Burkitt lymphoma cell lines, Ramos, Raji, Daudi and Namalwa, were purchased from the Japanese Collection of Research Bioresources (Tokyo, Japan). Hodgkin lymphoma cell lines, KM-H2, L-1236, L-540, L-428, HD-MY-Z, and HDLM-2, were purchased from Deutsche Sammlung Von Mikroorganismen und Zellkulturen (Braunschweig, Germany). The Hodgkin lymphoma cell line, DEV, was a kind gift from Professor S Poppema.[17] These cell lines were grown in RPMI 1640 supplemented with 10% heat-inactivated FCS at 37°C in 5% CO_2 in air.

Patients. Fifteen patients with PAL who were admitted to hospitals situated in the Osaka area, Japan, during the period from 1995 to 2003 were selected for the present study. Informed

[3]To whom correspondence should be addressed. E-mail: takakuwa@molpath.med.osaka-u.ac.jp

Abbreviations: EBV, Epstein–Barr virus; DAPI, 4′,6-diamidine-2′-phenylindole dihydrochloride; FCS, fetal calf serum; FISH, fluorescence *in situ* hybridization; HPLC, high-performance liquid chromatography; hTERT, telomerase catalytic subunit; PAL, pyothorax-associated lymphoma; PBS, phosphate-buffered saline; PNA, peptide nucleic acid; Rb, retinoblastoma; RPMI, Roswell Park Memorial Institute; RT-PCR, reverse transcription-polymerase chain reaction; SDS-PAGE, sodium dodecyl sulfate-polyacrylamide gel electrophoresis; TBS, Tris-buffered saline; TL, telomere length; UC, ulcerative colitis.

doi: 10.1111/j.1349-7006.2007.00482.x

consent was obtained from all patients. The age of the patients at first admission for PAL ranged from 65 to 82 (median, 72.0) years, with a male to female ratio of 10:5. Histologic specimens obtained using biopsy or surgery were fixed in 10% formalin, and routinely processed for paraffin embedding. Histologic sections, cut at 4 μm, were stained with H&E and treated with the immunoperoxidase procedure. Tumors were histologically classified as diffuse large B-cell lymphoma (immunoblastic variant 13 cases, centroblastic variant two cases) according to the World Health Organization classification. All cases prove to be positive EBER-1 expression of EBV using *in situ* hybridization. Genomic DNA was extracted from fresh frozen tumor biopsy samples and peripheral blood from three patients from whom the cell lines (OPL-3, -5, -7) were established.

Terminal restriction fragment TL analysis. The TL in the PAL cell lines and corresponding clinical samples was measured with Southern blot hybridization. A 6 μg sample of genomic DNA from each cell line and clinical samples was digested for 16 h with an RsaI/HinfI restriction enzyme mixture (Roche Diagnostics) at 37°C, and subjected to 0.8% agarose gel electrophoresis. The DNA was then transferred from the gel to a positively charged nylon membrane. Hybridization was carried out with 3-end digoxigenin-labeled $d(TAGGG)_5$ at 42°C for 16 h. Chemiluminescent detection was performed with ECL+ plus (GE Healthcare Bio-Sciences Corp., Piscataway, NJ, USA). Exposure of X-ray film to the membrane displayed telomere signals as smears.

FISH for detection of the telomere repeats. The PNA probe for telomeric sequences is included in the Telomere PNA FISH Kit/Cy3 (DakoCytomation, Glostrup, Denmark). The PNA centromeric probe/Cy3 for chromosome 2 was generated using DAKOCytomation,[18] which was added to the telomere probe solution, resulting in a final concentration of 2 ng/μL. Metaphase cells were collected after 2 h incubation with 4 μL/mL Colcemid (Sigma, St Louis, MO, USA), incubated with 75 mM KCl in 37°C for 20 min, fixed in 3:1 (v/v) HPLC-grade absolute methanol/glacial acetic acid, and mixed well gently before spreading onto slides. The hybridization was performed according to the manufacturer's instructions. In brief, this procedure included the following steps: slides were washed twice with TBS buffer (pH 7.5), treated with proteinase K for 10 min at room temperature, fixed in ethanol and air-dried. PNA probes were denatured together with the slide at 80°C for 3 min and hybridized for 30–60 min at room temperature. After extensive washing first at 65°C and then at room temperature, the slides were counterstained with DAPI and mounted with antifade solution (Vector Laboratories, Burlingame, CA, USA). The fluorescence signals in the metaphase-spread images were observed using a Carl Zeiss epifluorescence microscope (Axioplan 2 imaging, Germany) equipped with a HBO 100 mercury lamp and filters for DAPI and Cy3. The images were captured using a Sensys 1400 CCD camera (Photometrics, Berkeley, CA, USA). Camera control and digital image acquisition was performed using IP lab 3.1 software (Signal Analytics Corp, Vienna, VA, USA).

Pictures were taken at 1000 ms for the Cy3 images and 200 ms for the DAPI images. Normally, the metaphase-spread chromosome has four telomeres at each end. Occasionally one or some telomere signals were not detected in this condition, suggesting the telomere to be extremely short or deleted, that is, 'erosion' has occurred. 'Telomere erosion' was defined as negative when four telomere signals were detected on one chromosome in metaphase, and positive when less than four telomere signals were detected. The ratio of telomere erosion per each cell was calculated as the number of telomere erosion positive chromosomes/total number of chromosomes of each cell. The ratio of intrachromosomal signals was calculated as the number of intrachromosomal signal positive chromosomes/total number of chromosomes of each cell. For telomere signals counting, 20 metaphase cells were analyzed per slide. Experiments were done in triplicate. Cells containing no Cy3 signals were excluded from further analysis.

Detection of telomerase activity. Telomerase activity was measured using Quantitative Telomerase Detection kit (Allied Biotech, Inc, Karlsruhe, Germany) according to the manufacture's protocol. Briefly, 5×10^5 cultured cells washed with PBS were incubated in lysed buffer for 30 min on ice. Telomere templates were formed by adding 6-base-repeats to primer with the activity of telomerase in QTD mixture at 25°C for 20 min. RT-PCR assay was performed with an ABI Prism 7700 Sequence Detector System (Applied Biosystems). The thermocycling conditions were 95°C for 10 min for activation of Taq DNA polymerase, 40 cycles of denaturation at 95°C for 30 s, annealing at 60°C for 30 s, and extension at 72°C for 30 s.

Western blotting. Whole cultured cells were lysed by sonication in a buffer containing 15 mM Tris-HCl (pH 6.8), 10% glycerol, 2% SDS, and 6% β-mercaptoethanol. Following incubation at 95°C for 10 min, equal volume of protein extracts were separated with 15% SDS-PAGE for detection of $p16^{INK4a}$ and p53 and with 8% SDS-PAGE for Rb and hTERT protein, and then blotted to polyvinylidene difluoride membrane using a wet-blotting apparatus. Blots were blocked in PBS containing 0.05% Tween 20 and 1% non-fat dry milk, and incubated with each antibody at room temperature for 1 h. Antibodies used were antip16^{INK4a} (clone 16P04; Laboratory vision, Fremont, CA, USA), anti-Rb (clone IF8; Laboratory vision), antiphospho-Rb (Ser-795), phospho-Rb (Ser-780), phospho-Rb (Ser-807/811) (cell signaling, MA), anti-p53 (DO-7; DAKO), anti-hTERT (Rockland, Gilbertsville, PA, USA), and anti-actin (Sigma-Aldrich, Steinheim, Germany), respectively. Rb control proteins with and without phosphorylation *in vitro* by cdc2/cyclinB were purchased from cell signaling. Signals were visualized with ECL plus chemiluminescent reagents (GE Healthcare Bio-Sciences Corp.).

Immunohistochemistry. Immunohistochemical detection (avidin–biotin–peroxidase complex method) of $p16^{INK4a}$ and Rb protein expression was performed on the paraffin-embedded sections from the original tumor specimens as well as the established cell lines. Specimens from colon cancers were used as positive controls for $p16^{INK4a}$ and Rb protein detection.

Isolation of DNA and total RNA, RT-PCR, and detection of p53 mutations. DNA and total RNA were extracted from the cell lines with the TRIzol reagent (Invitrogen, Carlsbad, CA, USA). 5 μg of total RNA were reverse-transcribed with random hexamer priming using the Superscript first strand synthesis system (Invitrogen) according to the manufacturer's instructions. RT-PCR was performed to amplify the sequence spanning exon 5–8 of p53 (GenBank accession number NM000546; nt. 626–1170) using the following primer pair; 5′-GTACTCCCCTGCCCTCAACA-3′ and 5′-ACCTCGCTTAGTGCTCCCTG-3′. After electrophoresis on 2.0% agarose gel, DNA fragments were excised and purified using the Wizard SV gel extraction kit (Promega Co., WI, USA). DNA was directly sequenced using the purified DNA fragments as template and appropriate primers. Sequencing was performed by the dideoxy chain termination method using a DNA sequencing kit (Applied Biosystems) and the ABI PRISM 310 Genetic Analyzer. When two different products were amplified, they were cloned into pGEM-T easy plasmid vector and both products were sequenced. Mutations were confirmed using genomic DNA as a template. PCR was performed with the primer pairs described elsewhere.[19]

Bisulfite sequencing. Before bisulfite PCR analysis, untreated DNA was sequenced to confirm the CpG sites in the samples. All DNA samples underwent bisulfite sequencing to investigate the distribution and density of methylated CpG sites. Samples were subjected to bisulfite modification with the CpGenome DNA Modification Kit (Millipore, Billerica, MA, USA). Bisulfite sequencing of $p16^{INK4A}$ was performed according to the method

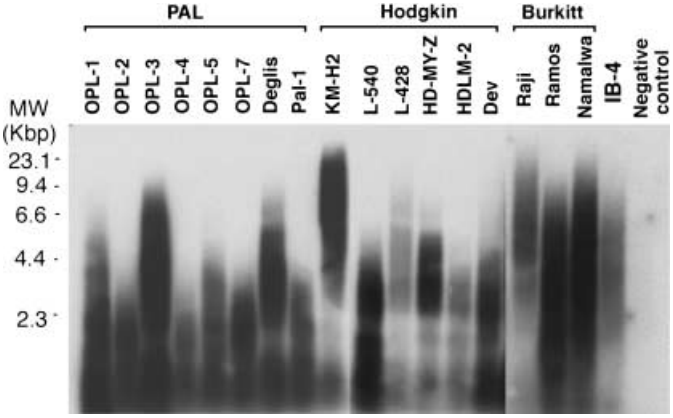

Fig. 1. Telomere length (TL) of cell lines was measured with Southern blot hybridization. Telomere sequence was detected with DIG-11-dUTP 3′ endlabeled $(TTAGGG)_5$ oligonucleotide probe. TL was shorter than 4.5 kbp in all pyothorax-associated lymphoma (PAL) cell lines. TL of Burkitt lymphoma cell lines was longer than that of PAL cell lines.

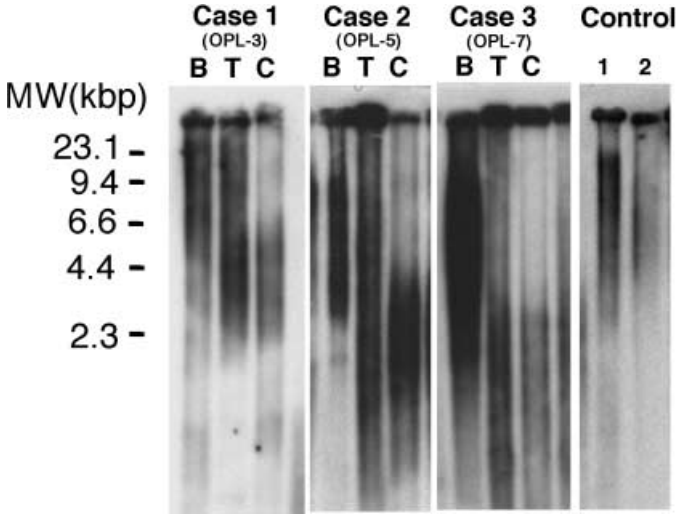

Fig. 2. Southern blot hybridization with DIG-11-dUTP 3′ endlabeled $(TTAGGG)_5$ oligonucleotide probe. Genomic DNA from peripheral blood leukocytes (B), tumors (T), and established cell lines (C) from pyothorax-associated lymphoma (PAL) patients were studied. Genomic DNA extracted from peripheral blood leukocytes from two healthy volunteers was used as a control. Telomere length showed a wide range in tumor tissues, but was shorter in PAL cell lines than in matched peripheral blood.

reported by Sato *et al*.[20] and Sakuma *et al*.[20,21] with amplification of a 384 bp product containing 35 CpG sites. PCR products were gel-purified using the Wizard SV gel extraction kit (Promega) and cloned into the pGEM-T easy plasmid vector. Six clones/cell lines were sequenced as described above.

Statistical analysis. Comparisons were made using Student's *t*-test (unpaired): *P*-values less than 0.05 were taken as statistically significant.

Results

Terminal restriction fragment telomere length analysis. TL in PAL cell lines was analyzed using Southern blotting. TL was extremely short, shorter than 4.5 kbp in all PAL cell lines: the mean TL were 2.3 kbp, 2.0 kbp, 4.5 kbp, 1.8 kbp, 2.3 kbp, 2.1 kbp, 4.0 kbp, and 2.1 kbp in OPL-1, -2, -3, -4, -5, -7, Deglis, and Pal-1, respectively (Fig. 1). TL in Hodgkin lymphoma cell lines was relatively short, except in KM-H2: 12.0 kbp, 2.5 kbp, 3.5 kbp, 3.3 kbp, 2.6 kbp, and 2.5 kbp in KM-H2, L-540, L-428, HD-MY-Z, HDLM-2, and DEV, respectively. TL of Burkitt lymphoma cell lines was longer than that of PAL cell lines: mean TL was 7.5 kbp, 5.0 kbp, 6.0 kbp, and 3.5 kbp in Raji, Ramos, Namalwa, and Daudi, respectively.

To examine whether telomere shortening is also observed in the original tumors, TL in leukocytes of peripheral blood from PAL patients and normal volunteers, tumor biopsy samples of PAL, and three cell lines (OPL-3, OPL-5 and OPL-7) was measured. TL in leukocytes from PAL patients was comparable with those from healthy volunteers (Fig. 2), and TL showed a wider range in tumor samples and was shorter than in the peripheral blood leukocytes from the matched patients. A wide range of TL in tumor tissue samples might be due to contamination of adjacent non-tumor tissues.

Telomere erosion in PAL cell lines. The mean TL was short and the range of telomere signal was broad in the PAL cell lines, which give rise to the question of whether telomeres are frequently erosive in PAL cell lines. In this connection, the telomere of each chromosome was detected using FISH analysis. Centromere for chromosome 2 used as an internal control was detected with high intensity in all cell lines (Fig. 3a). Telomere signal was detected with extremely low intensity in OPL-5. As shown in OPL-3, OPL-7 and Deglis (Fig. 3a), one of the telomeres in chromosome 2 was not detected in this condition, suggesting that the telomere was extremely short or deleted, that is, 'erosion' had occurred.

Then, the number of telomeres per each chromosome was counted in each cell line. Fig. 3b shows the representative telomere-FISH image obtained from IB4 and OPL-5 cell lines. In IB-4, 39 of 46 total chromosomes have four telomere signals, while seven (15.2%) have three signals. In OPL-5, only 23 of 40 chromosomes have four signals, and 16 (40%) chromosomes have less than three telomere signals, showing the frequent occurrence of telomere erosion (Fig. 3c).

The frequency of telomere erosion was compared between the cell lines (Fig. 4). Frequency of the telomere erosion was significantly higher in OPL-2 (mean percentage ± SD; 29.8 ± 11.9), OPL-5 (38.1 ± 14.9) and OPL-7 (26.7 ± 10.9) than in IB-4 (14.1 ± 10.2) and Namalwa (21.1 ± 11.2). The frequency of telomere erosion was not different between OPL-3 (13.4 ± 7.6), Deglis (17.5 ± 9.3), and IB-4.

Detection of telomerase activity. The regulation of telomerase is executed primarily through the transcriptional control of the gene encoding the catalytic subunit hTERT.[22,23] Most human somatic cells lack hTERT mRNA and telomerase activity, thus exhibiting telomere shortening as a sequel of cell division. Western blotting revealed that hTERT proteins were detected in all the PAL cell lines and Burkitt lymphoma cell lines examined (Fig. 5a). In addition, all PAL cell lines had telomere activities (Fig. 5b). Although telomere activity was relatively strong in OPL-1 and weak in OPL-7, no correlation between TL and telomere activity was observed. The mean telomerase activity in eight PAL lines was not significantly different from that in Burkitt lymphoma cell lines, Raji Ramos and Namalwa. These findings demonstrated that short TL in PAL cell lines did not result from weak/no telomerase activity.

Expression of $p16^{INK4a}$, Rb, and p53, and *p53* gene mutations. Telomere shortening usually induces cellular senescence, that is, arrest of proliferation via the $p16^{INK4a}$/Rb and/or $p14^{ARF}$/p53 pathways. In this respect, $p16^{INK4a}$, Rb, and p53 expressions together with *p53* mutations were analyzed.

Three of eight PAL cell lines (OPL-1, OPL-4, Deglis) expressed Rb using western blotting (Fig. 6a). Three phospho-Rb antibodies which detect at the three targeted sites (Ser-780,

doi: 10.1111/j.1349-7006.2007.00482.x

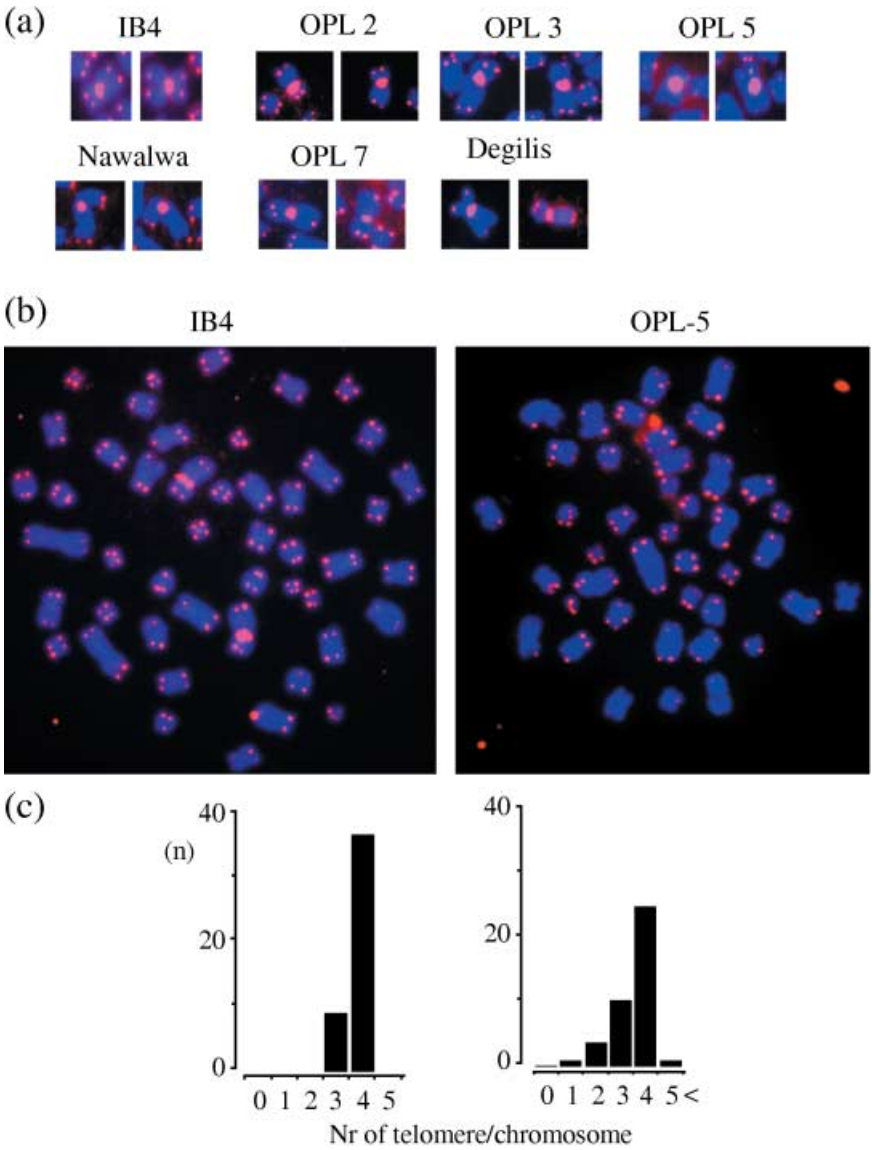

Fig. 3. (a) Representative fluorescence in situ hybridization (FISH) image for detection of telomere and centromere for chromosome 2 in five pyothorax-associated lymphoma (PAL) cell lines. Telomere signals in PAL cell lines were smaller in size than those in IB-4. Telomere was faint in OPL-5. One telomere in chromosome 2 was not detected in OPL-3 and OPL-7, suggesting that the telomere was extremely short or deleted, that is, 'erosion' had occurred. (b) Representative FISH analysis with PNA-Cy_3 telomere probes in OPL-5 and IB4 cell line. (c) The number of telomere signals/chromosome was counted from (b). Many chromosomes had telomere signals less than four in OPL-5 compared with IB-4.

-795, and -807/811, respectively) revealed that Rb protein expressed in three PAL cell lines (OPL-1, OPL-4 and Deglis) was heavily phosphorylated (Fig. 6b).

The PAL cell lines never expressed $p16^{INK4a}$ (Fig. 6a). Because the promoter methylation correlated well with repression of $p16^{INK4a}$, the methylation density of the regions was further investigated. A total of 48 clones in samples from the eight cell lines were sequenced, and the methylation status at 34 CpG sites in the region was analyzed (Fig. 6c). Of a total of 1632 sites examined, 1355 (83.0%) were methylated. CpG sites at position 11, 13, 14, 15, 17, 18, 19 were methylated in all clones examined. These results indicated that $p16^{INK4a}$ was transcriptionally inactivated by the promoter methylation in PAL cell lines.

$p16^{INK4a}$ and Rb expression was also shown to be frequently impaired in biopsy samples from PAL patients using immunohistochemistry. None (0%) and four (26.7%) of 15 cases expressed $p16^{INK4a}$ and Rb, respectively (data not shown). The methylation status at the p16 promoter region was analyzed in four cases (Fig. 6c). Of a total of 816 sites examined, 677 (83.0%) were methylated, indicating that $p16^{INK4a}$ was transcriptionally inactivated by promoter methylation in the clinical samples as well as the PAL cell lines.

A high frequency of p53 mutations in clinical specimens from PAL tissues (14 of 21 cases, 67%) has been previously reported.[19] Among the PAL cell lines, p53 protein expression was not detected in one cell line (OPL-5), was weak in one (OPL-3) and was small in size in one (OPL-2). Sequencing spanning from exon 5–8 of p53, which includes 'mutation hotspots', revealed mutations in four of eight PAL lines. Missense mutations were detected in three cell lines (OPL-1, OPL-4, Pal-1) and a frameshift mutation in one cell line (OPL-5). Missense mutations involved codon 246 (ATG→GTG; Met→Val) in OPL-1, codon 262 (GGT→GAT; Gly→Asp) in OPL-4, and codon 154 (GGC→AGC; Gly→Ser) in Pal-1 (GenBank accession number NM000546), respectively. In OPL-5, 16 bp deletions were found in exon 6. No deletions were detected between exon 5 and 8 in OPL-2. OPL-1 and OPL-5 had homozygous, while Pal-1 and OPL-4 had heterozygous mutations.

Discussion

Genome instability plays an important role in cancer development by accelerating the accumulation of the genetic changes responsible for cancer cell proliferation and survival. One of the

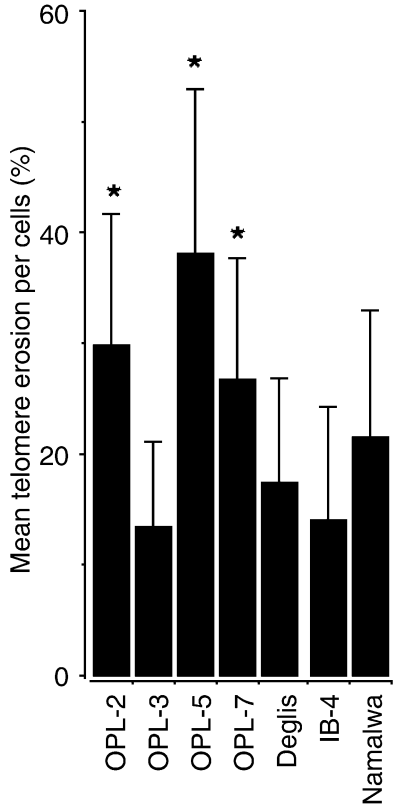

Fig. 4. Mean telomere erosion per cell was significantly higher in OPL-2, -5, and -7 than in IB-4 and Namalwa cell line.

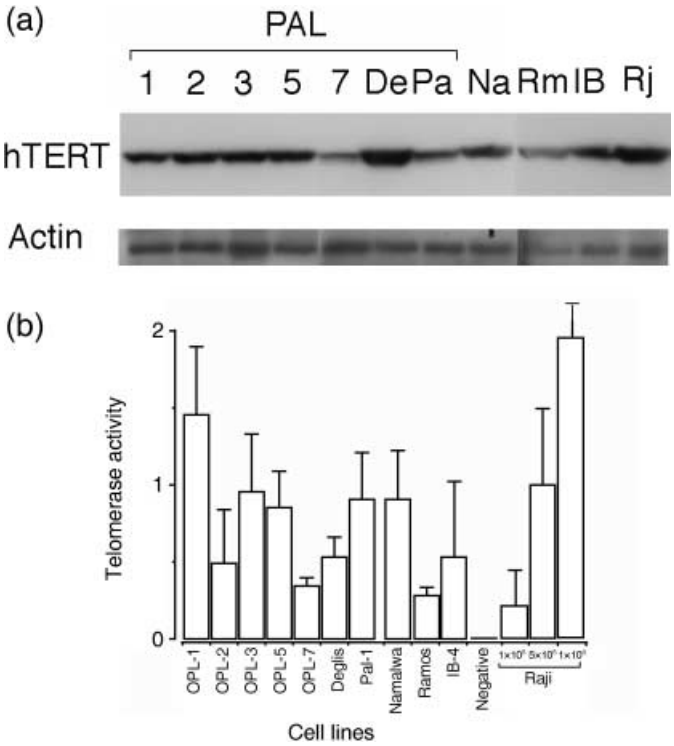

Fig. 5. (a) Western blotting revealed the expression of telomerase catalytic subunit (hTERT) proteins in all pyothorax-associated lymphoma (PAL) cell lines and Burkitt lymphoma cell lines examined. (b) Quantitative analysis of telomerase activity of PAL cell lines. Telomere activity in 5×10^5 cells of Raji was defined as 1.0 for comparison. Telomere activity was correlated with the cell number/sample in Raji cells.

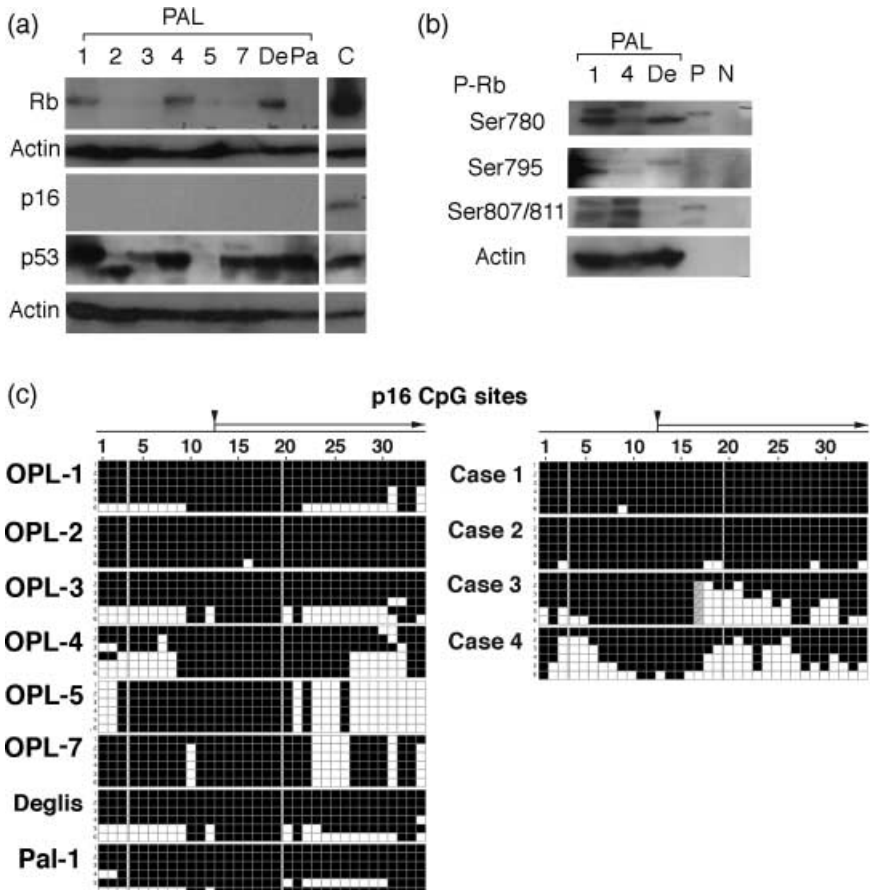

Fig. 6. (a) Retinoblastoma (Rb), $p16^{INK4a}$, and p53 protein expression in pyothorax-associated lymphoma (PAL) cell lines. Western blotting analysis revealed that $p16^{INK4a}$ and Rb expression was found in none and three (OPL-1, OPL-4 and Deglis) of eight PAL cell lines, respectively. p53 protein was not expressed in OPL-5, weakly expressed in OPL-3, and expressed but small in size in OPL-2. IB-4 was used as control for p53 and $p16^{INK4a}$ proteins while Jurkat was used for Rb protein. Anti-actin labeling showed equivalence of loading of cell lysates. 1: OPL-1, 2: OPL-2, 3: OPL-3, 4: OPL-4, 5: OPL-5, 7: OPL-7, De: Deglis, Pa: Pal-1, C: control. (b) Three phospho-Rb antibodies, which detect the targeted sites, revealed that Rb proteins expressed in three PAL cell lines (OPL-1, OPL-4 and Deglis) were heavily phosphorylated. Rb control proteins with and without phosphorylation *in vitro* by cdc2/cyclinB were provided in lanes (P) and (N), respectively. 1: OPL-1, 4: OPL-4, De: Deglis. (c) Methylation status of the *p16* gene promoter in PAL cell lines and clinical cases. A 384 bp product containing 34 CpG sites was amplified. 16 CpG sites reported previously correspond to sites 4–19.[20,21] Transcription start sites are shown by arrow heads. (■) Methylated CpG, (□) unmethylated CpG. Transcription start site are shown by arrow heads.

doi: 10.1111/j.1349-7006.2007.00482.x

well-known mechanisms for genome instability is telomere dysfunction. Telomeres are DNA–protein complexes that protect the ends of chromosomes and prevent chromosome fusion.[9]

TL is reported to be relatively short in hematopoietic malignancies such as acute/chronic myelogenous leukemia, acute/chronic lymphocytic leukemia, non-Hodgkin and Hodgkin lymphomas.[24] The mean TL in non-Hodgkin lymphomas of B-cell type has been reported to be 5.4 ± 0.7 kbp.[25,26] The TL in the PAL cell lines was extremely short; less than 4.5 kbp. The intensity of telomere signals as revealed using FISH with PNA probe was weak or unrecognizable, indicating frequent erosion of the telomere, while telomerase was reactivated. Intra-chromosomal telomere signals, which are indicative of the occurrence of telomeric fusion, were occasionally observed. TL in clinical samples of PAL showed a wide range compared to those in the corresponding cell lines. An explanation for this might be: (i) the concomitance of tumor tissues and adjacent non-tumor tissues; or (ii) the occurrence of telomere shortening in chronically inflamed tissues, underlying chronic pyothorax in the present case. Cells under such circumstances actively proliferate and are exposed to oxidative injuries. A similar situation is found in colorectal cancer arising in UC. O'Sullivan *et al*. have reported telomere shortening in UC, and its correlation with genome instability and a high frequency of anaphase bridges.[27] The telomere shortening in chronic inflammation might result in genome instability, which finally leads to carcinogenesis. The telomere shortening in primary human cells leads to replicative senescence, which is controlled by a $p14^{ARF}$/p53 and $p16^{INK4a}$/Rb pathway.[8,9,28] A recent study has demonstrated that replicative senescence is an important tumor suppressor mechanism.[29,30] Oncogene-induced senescence is a cellular response that may be crucial for protection against cancer development.[29,30] In premalignant tumors, senescence-related proteins are up-regulated.[31] In the PAL cell lines as well as the tumor biopsy samples, p53, $p16^{INK4a}$ and Rb proteins were inactivated, which allows continuous cell division. The inactivation rate of $p16^{INK4a}$ and Rb in PAL was much higher than that previously reported for other kinds of diffuse large B-cell lymphomas.[32]

Inhibition of the $p14^{ARF}$/p53 and/or the $p16^{INK4a}$/Rb pathway allows continuous cell division and critical telomere shortening, known as 'telomere crisis'. Telomeres are no longer able to perform their protective capping function under this condition, which results in chromosome end-to-end fusions, thus generating dicentric and ring chromosomes that often break or missegregate during mitosis.[33] The resultant broken ends can undergo additional rounds of recombination, forming complex chromosome rearrangements and aneusomies.[34,35] It has been postulated that such dysfunctional telomeres may promote neoplastic transformation through induction of genome instability, therefore playing a causal role in tumorigenesis.[9,36]

The TL in PAL cell lines was extremely short, although telomerase in these lines was reactivated to a similar level to that in Burkitt lymphoma cell lines. Telomerase activity in Burkitt lymphoma was significantly higher than that in other types of non-Hodgkin lymphomas.[37] Therefore telomerase activity in PAL cell lines may be enough to maintain telomere functions. A recent study has demonstrated that the DNA damage response proteins such as ATM, NBS1-RAD50-MRE11 complex, and Ku are involved in telomere maintenance.[38] Accelerated telomere shortening has been reported in patients with ataxia telangiectasia.[39] The authors' previous study showed heterozygous mutations of *ATM* in five of eight cell lines (OPL-1, OPL-3, OPL-4, OPL-5, and Pal-1);[40] among them OPL-1, OPL-4, OPL-5 and Pal-1 showed extremely short telomeres, suggesting that mutations of ATM might be involved in the rate of telomere shortening in PAL development and/or maintenance of the short telomeres even after reactivation of telomerase.

Taken together, telomere dysfunction and inactivation of the $p16^{INK4a}$/Rb pathway might play a role for PAL development. It is well known that non-Hodgkin lymphomas frequently develop in the organs affected by chronic inflammation, which encompasses malignant lymphoma of mucosa-associated lymphoid tissue (MALT) type. PAL differs to such lymphomas in that PAL is intimately related to EBV infection.[1] It will be interesting to know whether similar mechanisms as explained above for PAL development also work in MALT lymphoma.

Acknowledgments

We thank Dr Daibata, Dr Al Saati, and Dr Kieff for providing us the Pal-1, Deglis and IB-4, respectively. We thank DakoCytomation (Glostrup, Denmark) for providing us the PNA centromeric probe/Cy3 for chromosome 2. This study was supported by grants from the Ministry of Education, Science, Culture, and Sports, Japan (15026209, 15406013, 15590340, 16390105, 18014015).

References

1 Nakatsuka S, Yao M, Hoshida Y, Yamamoto S, Iuchi K, Aozasa K. Pyothorax-associated lymphoma: a review of 106 cases. *J Clin Oncol* 2003; **20**: 4255–60.
2 Iuchi K, Aozasa K, Yamamoto S *et al*. Non-Hodgkin's lymphoma of the pleural cavity developing from long-standing pyothorax. Summary of clinical and pathological findings in thirty-seven cases. *Jpn J Clin Oncol* 1989; **19**: 249–57.
3 Banks PM, Harris NL, Warnke RA, Gaulard Ph. Lymphomas. In: Travis WD, Brambilla E, Mueller-Hermelink HK, Harris CC, eds. *World Health Organization Classification of Tumors: Pathology and Genetics of Tumors of the Lung, Pleura, Thymus and Heart*. Lyon: IARC Press, 2004: 137–40.
4 Kanno H, Yasunaga Y, Ohsawa M *et al*. Expression of Epstein-Barr virus latent infection genes and oncogenes in lymphoma cell lines derived from pyothorax-associated lymphoma. *Int J Cancer* 1996; **67**: 86–94.
5 Takakuwa T, Luo WJ, Ham MF, Mizuki M, Iuchi K, Aozasa K. Establishment and characterization of unique cell lines derived from pyothorax-associated lymphoma which develops in long-standing pyothorax and is strongly associated with Epstein-Barr virus infection. *Cancer Sci* 2003; **94**: 858–63.
6 Blackburn EH. Switching and signaling at the telomere. *Cell* 2001; **106**: 661–73.
7 Moyzis RK, Buckingham JM, Cram LS *et al*. A highly conserved repetitive DNA sequence, (TTAGGG)n, present at the telomeres of human chromosomes. *Proc Natl Acad Sci USA* 1988; **85**: 6622–6.
8 Artandi SE, DePinho RA. A critical role for telomeres in suppressing and facilitating carcinogenesis. *Curr Opin Genet Dev* 2000; **10**: 39–46.
9 Ohtani N, Yamakoshi K, Takahashi A, Hara E. The $p16^{INK4a}$-RB pathway: molecular link between cellular senescence and tumor suppression. *J Med Invest* 2004; **51**: 146–53.
10 Meeker AK, Hicks JL, Platz EA *et al*. Telomere shortening is an early somatic DNA alteration in human prostate tumorigenesis. *Cancer Res* 2002; **62**: 6405–9.
11 Zhang A, Wang J, Zheng B *et al*. Telomere attrition predominantly occurs in precursor lesions during in vivo carcinogenic process of the uterine cervix. *Oncogene* 2004; **23**: 7441–7.
12 Gisselsson D, Jonson T, Petersen A *et al*. Telomere dysfunction triggers extensive DNA fragmentation and evolution of complex chromosome abnormalities in human malignant tumors. *Proc Natl Acad Sci USA* 2001; **98**: 12 683–8.
13 Chadeneau C, Hay K, Hirte HW, Gallinger S, Bacchetti S. Telomerase activity associated with acquisition of malignancy in human colorectal cancer. *Cancer Res* 1995; **55**: 2533–6.
14 al Saati T, Delecluze HJ, Chittal S *et al*. A novel human lymphoma cell line (Deglis) with dual B/T phenotype and gene rearrangements and containing Epstein-Barr virus genomes. *Blood* 1992; **80**: 209–16.
15 Daibata M, Taguchi T, Nemoto Y *et al*. Epstein-Barr virus (EBV)-positive pyothorax-associated lymphoma (PAL): chromosome integration of EBV in a novel CD2-positive PAL B-cell line. *Br J Haematol* 2002; **117**: 546–57.
16 King W, Thomas PA, Raab TN, Hawke M, Kieff E. Epstein-Barr virus RNA. V. Viral RNA in a restringently infected, growth-transformed cell line. *J Virol* 1980; **36**: 506–18.
17 van den Berg A, Kroesen BJ, Kooistra K *et al*. High expression of B-cell receptor inducible gene BIC in all subtypes of Hodgkin lymphoma. *Genes Chromosomes Cancer* 2003; **37**: 20–8.

18 Perner S, Bruderlein S, Hasel C *et al*. Quantifying telomere lengths of human individual chromosome arms by centromere-calibrated fluorescence in situ hybridization and digital imaging. *Am J Pathol* 2003; **163**: 1751–6.
19 Hongyo T, Kurooka M, Taniguchi E *et al*. Frequent p53 mutations at dipyrimidine sites in patients with pyothorax-associated lymphoma. *Cancer Res* 1998; **58**: 1105–7.
20 Sato M, Horio Y, Sekido Y, Minna JD, Shimokata K, Hasegawa Y. The expression of DNA methyltransferases and methyl-CpG-binding proteins is not associated with the methylation status of $p14^{ARF}$, $p16^{INK4A}$ and RASSF1A in human lung cancer cell lines. *Oncogene* 2002; **21**: 4822–9.
21 Sakuma K, Chong JM, Sudo M *et al*. High-density methylation of $p14^{ARF}$ and $p16^{INK4A}$ in Epstein-Barr virus-associated gastric carcinoma. *Int J Cancer* 2004; **112**: 273–8.
22 Meyerson M, Counter CM, Eaton EN *et al*. hEST2, the putative human telomerase catalytic subunit gene, is up-regulated in tumor cells and during immortalization. *Cell* 1997; **90**: 785–95.
23 Nakamura TM, Morin GB, Chapman KB *et al*. Telomerase catalytic subunit homologs from fission yeast and human. *Science* 1997; **277**: 955–9.
24 Ohyashiki JH, Sashida G, Tauchi T, Ohyashiki K. Telomeres and telomerase in hematologic neoplasia. *Oncogene* 2002; **21**: 680–7.
25 Harada K, Kurisu K, Arita K *et al*. Telomerase activity in central nervous system malignant lymphoma. *Cancer* 1999; **86**: 1050–5.
26 Remes K, Norrback KF, Rosenquist R, Mehle C, Lindh J, Roos G. Telomere length and telomerase activity in malignant lymphomas at diagnosis and relapse. *Br J Cancer* 2000; **82**: 601–7.
27 O'Sullivan JN, Bronner MP, Brentnall TA *et al*. Chromosomal instability in ulcerative colitis is related to telomere shortening. *Nat Genet* 2002; **32**: 280–4.
28 Kiyono T, Foster SA, Koop JI, McDougall JK, Galloway DA, Klingelhutz AJ. Both $Rb/p16^{INK4a}$ inactivation and telomerase activity are required to immortalize human epithelial cells. *Nature* 1998; **396**: 84–8.
29 Serrano M, Lin AW, McCurrach ME, Beach D, Lowe SW. Oncogenic ras provokes premature cell senescence associated with accumulation of p53 and $p16^{INK4a}$. *Cell* 1997; **88**: 593–602.
30 Braig M, Lee S, Loddenkemper C *et al*. Oncogene-induced senescence as an initial barrier in lymphoma development. *Nature* 2005; **436**: 660–5.
31 Michaloglou C, Vredeveld LC, Soengas MS *et al*. BRAFE600-associated senescence-like cell cycle arrest of human naevi. *Nature* 2005; **436**: 720–4.
32 Moller MB, Kania PW, Ino Y *et al*. Frequent disruption of the RB1 pathway in diffuse large B cell lymphoma: prognostic significance of E2F-1 and $p16^{INK4A}$. *Leukemia* 2000; **14**: 898–904.
33 Counter CM. The roles of telomeres and telomerase in cell life span. *Mutat Res* 1996; **366**: 45–63.
34 Lundblad V, Szostak JW. A mutant with a defect in telomere elongation leads to senescence in yeast. *Cell* 1989; **57**: 633–43.
35 Blasco MA, Lee HW, Hande MP *et al*. Telomere shortening and tumor formation by mouse cells lacking telomerase RNA. *Cell* 1997; **91**: 25–34.
36 Hastie ND, Allshire RC. Human telomeres: fusion and interstitial sites. *Trends Genet* 1989; **5**: 326–31.
37 Klapper W, Krams M, Qian W, Janssen D, Parwaresch R. Telomerase activity in B-cell non-Hodgkin lymphomas is regulated by hTERT transcription and correlated with telomere-binding protein expression but uncoupled from proliferation. *Br J Cancer* 2003; **89**: 713–19.
38 Slijepcevic P. The role of DNA damage response proteins at telomeres-an 'integrative' model. *DNA Repair* 2006; **22**: 1299–306.
39 Metcalfe JA, Parkhill J, Campbell L *et al*. Accelerated telomere shortening in ataxia telangiectasia. *Nat Genet* 1996; **13**: 350–3.
40 Liu A, Takakuwa T, Fujita S *et al*. Alterations of DNA damage-response genes ATM and ATR in pyothorax-associated lymphoma. *Lab Invest* 2005; **85**: 436–46.

doi: 10.1111/j.1349-7006.2007.00482.x